



PAPER

OPEN ACCESS

RECEIVED
2 September 2019

REVISED
30 November 2019

ACCEPTED FOR PUBLICATION
11 December 2019

PUBLISHED
14 January 2020

Original content from this work may be used under the terms of the [Creative Commons Attribution 3.0 licence](#).

Any further distribution of this work must maintain attribution to the author(s) and the title of the work, journal citation and DOI.



Self-powered, flexible and room temperature operated solution processed hybrid metal halide p-type sensing element for efficient hydrogen detection

E Gagaoudakis^{1,2,7} , A Panagiotopoulos^{3,4,7}, T Maksudov^{3,4,7}, M Moschogiannaki^{2,3}, D Katerinopoulou^{1,2}, G Kakavelakis^{3,5}, G Kiriakidis^{1,2}, V Binas^{1,2}, E Kymakis⁴ and K Petridis⁶

¹ Department of Physics, University of Crete, Heraklion, Greece

² Institute of Electronic Structure and Laser, Foundation for Research and Technology Hellas, 100 N. Plastira str., Vassilika Vouton, 70013 Heraklion, Crete, Greece

³ Department of Materials Science and Technology, University of Crete, GR-71003, Heraklion, Greece

⁴ Department of Electrical & Computer Engineering, Hellenic Mediterranean University, Estavromenos P.B 1939, Heraklion, GR-71 004, Crete, Greece

⁵ Cambridge Graphene Centre, University of Cambridge, 9 JJ Thomson Avenue, Cambridge CB3 0FA, United Kingdom

⁶ Department of Electronic Engineering, Hellenic Mediterranean University, Romanou 3, Chalepa, 73100, Chania, Crete, Greece

⁷ These authors contributed equally to the preparation of the manuscript.

E-mail: c.petridischania@gmail.com

Keywords: lead halide perovskites, self-powered hydrogen sensing element, solution processed, room temperature sensing, p-type sensing elements, sensitivity, flexible substrate

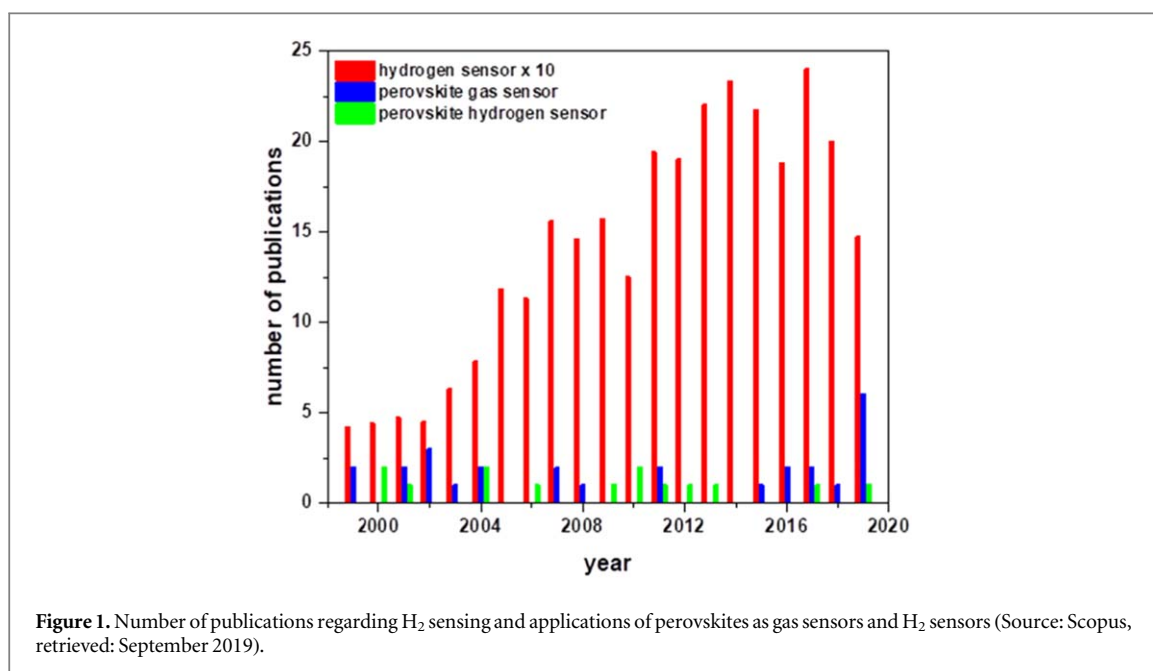
Abstract

Hydrogen (H₂) is a well-known reduction gas and for safety reasons is very important to be detected. The most common systems employed along its detection are metal oxide-based elements. However, the latter demand complex and expensive manufacturing techniques, while they also need high temperatures or UV light to operate effectively. In this work, we first report a solution processed hybrid mixed halide spin coated perovskite films (CH₃NH₃PbI_{3-x}Cl_x) that have been successfully applied as portable, flexible, self-powered, fast and sensitive hydrogen sensing elements, operating at room temperature. The minimum concentrations of H₂ gas that could be detected was down to 10 ppm. This work provides a new pathway on gases interaction with perovskite materials, poses new questions that must be addressed regarding the sensing mechanisms involved. The utilization of halide perovskite sensing elements demonstrates their potential beyond solar cell applications.

1. Introduction

Hydrogen (H₂) gas is expected to be a green (no emissions) and renewable energy source (with high heat combustion 142 kJ g⁻¹, minimum ignition energy 0.017 mJ and highly flammable range up to 75%) for many applications such as glassmaking, semiconductor processing, biomedical applications, seismic surveillance, fuel cells, automobiles, power generators and aerospace (liquid H₂ already been used for rocket fuels) [1, 2]. In the near future it could be used as a city gas or as a fuel to power cars in the same way as natural gas is leveraged. However, H₂ is an extremely dangerous gas since it is odourless, colourless, and highly flammable, with high burning velocities and its leakage poses explosion hazards (a lower explosion limit (LEL) at 40000 ppm) [3]. So, it is essential (see figure 1) to be detected reliably and fast, in low concentrations preferably below 100 ppm, for safety protection reasons [4–7].

A H₂ sensor could be a transducer that converts a variation of physical or chemical characteristic into an electrical current. A number of applications, including gas chromatography, mass spectrometry, thermal conductivity, laser-induced breakdown spectroscopy, scanning photoelectrochemical microscopy, and gas sensors, have been employed to detect hydrogen gas [8–14]. Among them, the hydrogen gas semiconductor-based sensors are being studied for their small size; low power consumption; high accuracy, reliability; fast response; and reliable/low cost fabrication processes [15]. Subject to the signal monitored, the H₂ sensing



elements can be divided into (a) resistance based; (b) work function based; (c) optical; and (d) acoustic elements. Figures of merit of an ideal sensing element are (a) the sensitivity to various targeted gas agents; (b) the selectivity between various targeted gases; (c) the fast response when exposed in the environment of the targeted gas; (d) reversibility to its initial pristine stage before the exposure to the targeted agent; (e) the efficient detection of the signal generated as a result of the interaction of the sensing element with the targeted gas; (f) the low cost and facile fabrication process; (g) stability and long life time (h) the operation at low temperature (ideally at room temperature), without the need of an external trigger (temperature or UV light) to provide sensing abilities.

In this paper, we will be focused on the modulation of the electrical resistance of the sensing element as a result of the adsorption and desorption of the H₂ gas molecules through it. The perovskite sensing element demonstrated a very promising performance towards H₂ gas sensing. The motivation originated from the fact that the most common employed H₂ sensing materials (metal oxides—SnO₂, ZnO, TiO₂, Nb₂O₅, In₂O₃, FeO, NiO, Fe₂O₃, Ga₂O₃, MoO₃, V₂O₅, WO₃) do not contain all the figures of merit of an ideal sensing element, despite their appealing characteristics: small size, high sensitivity, high repeatability and simplicity to use. Often, they suffer from some serious drawbacks such as (a) high operation temperatures (operation at room temperature has shown weak response to low concentration H₂ or have long response-recovery time; moreover, operating at high temperatures is very risky especially when the targeted gas is an explosive gas such as H₂); (b) they need a pre-treatment with UV light in order to become conductive; and (c) their fabrication is complicated and expensive (e.g. rf sputtering, dc sputtering, high vacuum facilities, pulsed laser deposition [16–21]).

Hybrid metal halide perovskite materials have attracted an enormous interest in the field of solar cell technology due to their fantastic physical properties. They follow the ABX₃ structure where, A is an organic cation usually methylammonium (MA⁺), formamidinium (FA⁺) or an inorganic cation such as Cs⁺, Rb⁺ and K⁺, B is a metal such as Pb²⁺, Sn²⁺, while the anion X is a halogen such as I⁻, Br⁻, Cl⁻ or a mixture thereof. The very first report on semiconductor halide perovskite was via observing photoconductivity in the all inorganic CsPbX₃ systems at late 1950' by Moller [22]. Later on, perovskite was used as absorbing material in photovoltaic applications by Kojima *et al* in 2009 [23]. In the last decade, the efficiency of perovskite based solar cells have been skyrocketed from 3.8% to higher than 25% [24]. The hybrid lead halide perovskites, such as the mixed halide one studied here (CH₃NH₃PbI_{3-x}Cl_x), have recently attracted the scientific communities' attention as one of the most promising solar light energy harvesting materials due to their direct band gap, long diffusion charge carrier lengths, large absorption coefficients, long carrier lifetime and large carrier mobility [25–27]. The impressive impact of perovskite in solar cell technology, have attracted an intensive research interests towards the applications of perovskites beyond solar cells such as in lasers [28] in light emitting diodes [29, 30] and photo-detectors [31, 32]. However, one of the key issues to be solved in order to boost their commercialization is related to their stability. Halide perovskites are very sensitive to polar gases and vapours, as, exposure to such elements deteriorates substantially and very fast the perovskite devices' performance. Turning this disadvantage to an advantage (regarding the sensing properties of these materials and not their lifetime under exposure of the targeted gases that sometimes is a challenge to be addressed in the near future) reflects the introduction of perovskite-based gas sensing elements. The sensitivity of perovskite to environmental gases is an opportunity to

convert a drawback to an opportunity [33]. Recently, halide perovskites have been explored and demonstrate their competence over the existed technologies, as potential sensing elements from gas molecules to x-ray photons [34–38]. Related literature regarding inorganic perovskites applications in H₂ sensing, have started to appear [39, 40] (figure 1) showing the potential of this family of materials towards hydrogen sensing. However, all reported inorganic perovskite materials need to operate at very high temperatures (of few hundred Celsius) in order to function as hydrogen sensors. In this paper, we introduce for the first time according to our knowledge, a solution processed hybrid metal halide perovskite film (CH₃NH₃PbI_{3-x}Cl_x), that requires much simpler fabrication and deposition techniques & facilities than the previously reported for other H₂ sensing element materials. Moreover, the performance characteristics of the demonstrated sensing element are not inferior to many of figures of merit of the other technologies reported. The perovskite-based sensing element presented here, demonstrated a very promising performance characteristics towards hydrogen sensing, i.e.: (a) operation at room temperature; (b) no requirement of an external optical signal to be switched on prior to its exposure into a hydrogen environment; (c) fast response time (few secs); (d) detection sensitivity with resolution down to 10 ppm; and (e) compatibility with flexible substrates. The aforementioned features make hybrid mixed halide perovskite semiconductors competitive (and beyond the simpler and of lower cost fabrication and deposition techniques) candidates to other already demonstrated in hydrogen sensing materials such as metal oxides and metals [4]. In particular, compared to metal oxides (e.g. SnO₂, ZnO, TiO₂, FeO, Fe₂O₃, NiO, Ga₂O₃, In₂O₃, Sb₂O₅, MoO₃ and WO₃) that request high temperatures to operate as hydrogen sensing elements, the demonstrated hybrid perovskite film operate in room temperature reducing a lot the consuming power. To highlight that the performance of both systems, regarding the reaction times (of the order of few seconds) and minimum detection limits, are similar (of the order of 10 ppm). Their advantages compared to metallic resistors (e.g. palladium & platinum metals) are: (a) request simpler deposition techniques (e.g. spin coating) compared to more complicated and expensive techniques the metallic resistors request: vacuum evaporation, electrode position, sputtering and pulsed laser deposition; (b) do not suffer from mechanical degradation when exposed to hydrogen environment and thus do not request complicated metallic alloys to address the issue of the mechanical degradation. We should also highlight that hybrid perovskite semiconductors, show similar minimum detection limits as metallic resistors.

The studied sensing films demonstrated a p-type semiconductor behaviour (attributed to its stoichiometry) and thus under H₂ gas (reducing gas) exposure their electrical resistance was enhanced upon H₂ exposure. However, its pristine electrical properties were restored very fast (within few secs) after the removal of the H₂ gas. This work sets the framework for further research of room temperature operated, efficient, of low cost, conductometric (resistance measurement), flexible halide perovskite H₂ sensing elements and systems. This is essential for various applications ranging from the energy sector to aerospace industry.

2. Methodology

To fabricate the CH₃NH₃PbI_{3-x}Cl_x precursor solution, methylammonium iodide (MAI, purchased by Dyesol) with lead (II) chloride (PbCl₂, 99.999% purchased by Sigma Aldrich) were mixed in a molar ratio of 3:1 within an anhydrous N,N dimethylformamide (DMF) solvent. The resulted solution (with 40 wt% concentration) was stirred using ultrasounds for 12 h and at 70 °C. Continuously the precursor solution was cooled down at room temperature and deposited (approximately 20 μl filtered precursor solution) onto the sensing element electrodes template (purchased from DropSens). The latter and prior to the spreading of the solution precursor, was UV ozone cleaned to remove any hazards (e.g. organic contaminants) that can lower its hydrophilicity. The electrode substrate was glass made and on top of the glass two interdigitated platinum electrodes were made. The distance between the electrodes was 5 μm. The deposited solution was spin-coated at 4000 rpm for 45 s. Afterward, the precursor solution spread over the electrodes was thermally annealed at 100 °C for 75 min to crystalline the CH₃NH₃PbI_{3-x}Cl_x hybrid perovskite semiconductor. The entire processing was conducted inside a nitrogen-filled glove box with O₂ and H₂O concentrations below 0.1 ppm. Prior to the checking of the sensing properties of the glass/Pt/CH₃NH₃PbI_{3-x}Cl_x sandwich elements, the latter were fully characterized as a function of their electronic, morphological, structural properties. The electrical connection of the active material with the electrodes was checked after the exposure of the glass/Pt/CH₃NH₃PbI_{3-x}Cl_x system in simulated solar light (A.M 1.5G at 100 mW cm⁻²) under ambient conditions (~45% relative humidity). The film roughness was examined using Atomic Force Microscopy (AFM), by employing a Park XE-7 instrument in tapping mode. The total scan area was set to 50 μm × 50 μm and the scan rate was fixed at 0.3 Hz. The successful crystallization of the hybrid CH₃NH₃PbI_{3-x}Cl_x perovskite semiconductor was assessed using a D/MAX-2000 x-ray diffractometer under monochromatic Cu Kα irradiation (λ = 1.5418 Å) at a scan rate of 4° min⁻¹. Whereas the grain size of the crystallized perovskite film was evaluated through scanning electron microscope (SEM, using the JEOL JSM-7000F) measurements.

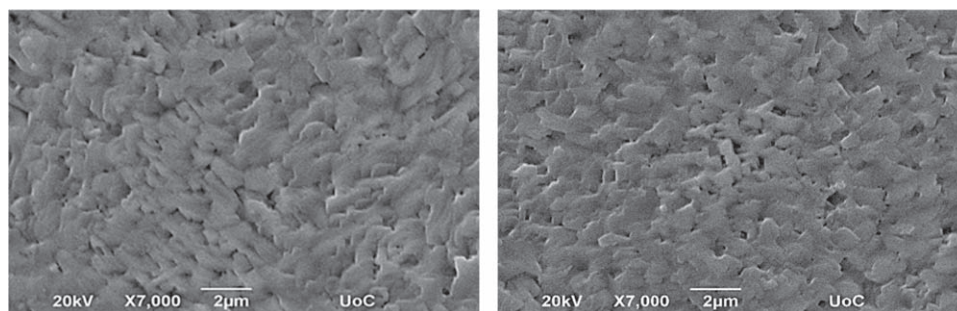


Figure 2. SEM image of the surface of the MHP employed as sensing element for hydrogen before (left image) and after (right image) exposure to hydrogen. No changes in the morphology were observed. Using the Scherrer equation the grain size was calculated to be of the order of 250 nm.

All the hydrogen sensing measurements occurred within a homemade gas test chamber under dark conditions in order to lower the rates of photoexcitation that contributes to dark current. Prior to the sensing test measurements that occurred, the electrical conductivity of our elements was tested. A potential difference of one Volt was applied across the two platinum electrodes of glass/Pt/CH₃NH₃PbI_{3-x}Cl_x systems and the induced generated current was measured using a Keithley 6517A multi-meter set-up. All these initial measurements were taken at room temperature and under a pressure of 1.6 mbar.

After the baseline of the conductivity of our sensing elements was measured, the CH₃NH₃PbI_{3-x}Cl_x sensors were exposed for five minutes to hydrogen gas at a constant flow of 500 sccm (standard cubic centimetres per minute), while the pressure in the chamber was kept constant at 120 mbar, leading to a decrease of current. The hydrogen concentrations that the detector was exposed were 100, 75, 50, 25, and 10 ppm (in synthetic air). The sensing performance of our sensing elements could not be assessed for hydrogen concentrations higher than 100 ppm for safety reasons. The CH₃NH₃PbI_{3-x}Cl_x sensor was exposed for time intervals of five minutes at each concentration, while another five minutes was given to the sensor to relax to its steady-state conditions.

3. Results

3.1. Structural, morphological and optical analysis

A 300 nm thick CH₃NH₃PbI_{3-x}Cl_x film was fabricated onto a glass substrate with prepatterned electrodes; the interdigitated electrodes made of platinum had distance between them of 5 µm. It must be highlighted at this point that the majority carriers within the perovskite semiconducting film are subject to the stoichiometry of the PbI²/MA⁺I precursor ratio; in our case this ratio was less than one and the film demonstrated a p-type semiconducting behaviour [41]. The entire fabrication process was performed inside a glovebox under nitrogen atmosphere.

The film's surface morphology controls the number of the provided interaction pathways that the targeted gas molecules can interact on with the sensing element; increased roughness, facilitates the gas molecules adsorption by providing longer diffusion lengths within the active material. The surface film's morphology was revealed using AFM measurements. AFM patents were taken before and after the exposure to H₂. A significant change in the AFM images was observed, with the roughness to reduce almost to its half value after the exposure to 100 ppm of hydrogen gas. The reason of this morphological change is thought to relate to the interaction of H₂-molecules with the perovskite surface species; however, the exact cause needs further investigation before it can be attributed to a specific factor. Subsequently, a slight decrease in the measured current (of the order of few nA during the measurement cycles) was attributed to the resulted smoother surfaces; the latter provide shorter percolations paths to allow the H₂ molecules to interact with the perovskite platform.

The SEM images of the employed mixed halide films reveal the well-shaped formed grains on its surface and the film's porosity. The existence of a porous surface on the film, facilitates the penetration and the evacuation paths of the hydrogen atoms through it (figure 2). The good conductivity of the film is very much linked with the grain size; using the Scherrer formula their size was measured of the order of 250 nm. The SEM images before and after the exposure to the H₂ gas revealed no substantial changes on the grain size.

The film's crystal structure was studied using the x-ray diffraction (XRD) technique. The successful crystallization of the spin coated perovskite film is depicted in the acquired XRD image (figure 3). The crystal directions of the first (110) and the second (220) crystallographic plane can be seen, at ~14.2° and ~28.5° respectively, confirming the, as expected, cubic perovskite phase [42]. No compositional changes were observed before and after the H₂ to hydrogen gas molecules (at 100 ppm for more than one hour), showing the sensing

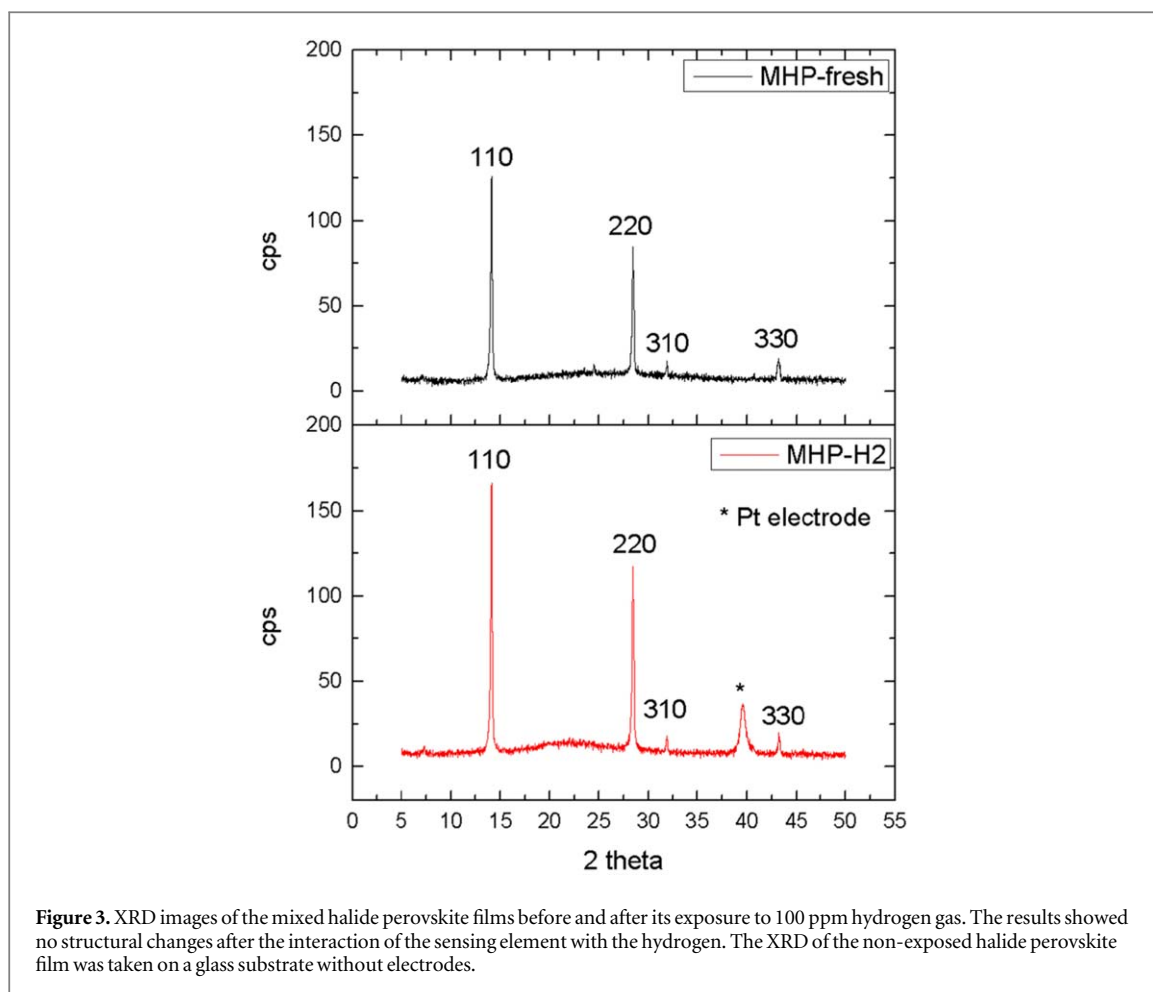


Figure 3. XRD images of the mixed halide perovskite films before and after its exposure to 100 ppm hydrogen gas. The results showed no structural changes after the interaction of the sensing element with the hydrogen. The XRD of the non-exposed halide perovskite film was taken on a glass substrate without electrodes.

potential and stability of the fabricated films. This is a clear indication that the interacted H_2 molecules just adsorbed and de-adsorbed through the perovskite-based template.

3.2. Sensing properties of the $CH_3NH_3PbI_{3-x}Cl_x$ thin films

The sensing functionality of the films on H_2 was examined by electrical measurements at room temperature that carried out in a homemade set-up. We exposed the aforementioned perovskite films to various H_2 gas concentrations up to the maximum of 100 ppm for safety reasons. Interruption the H_2 gas flow, restored the films' conductivity to their initial levels. The excellent electrical properties (long diffusion lengths, high charge mobility and excellent mobility to charge lifetime product), the interdigitated electrodes (Pt electrodes with distance of the order of $10\ \mu m$) setup and the application of a forward bias across the electrodes (0.5 and 1 V) allowed us to register (a) the current across the film (of the order of μA); and (b) its modulations when the film was exposed to H_2 environment. The report of such high currents (in μA range) through the film is an indication of its excellent electrical properties as a result of the long grain's size and high carrier's diffusion length of the $CH_3NH_3PbI_{3-x}Cl_x$ perovskite layer employed as sensing material. The demonstrated sensing elements were self-powered thus there was no the need of any external assistance such as UV irradiation or heating in high temperatures. H_2 molecules operated as a reducing gas, and since the exhibited perovskite film is a p-type semiconductor, lowering of the current was observed, as expected, caused by the adsorption of the H_2 molecules (the opposite behaviour than n-type semiconductors). Figure 4 depicts the current modulation for (a) various exposure times (one and five minutes); and (b) under different forward biases 0.1, 0.5 and 1 Volt.

During the sensing measurement process, the modulation of the current flowing through the film was recorded, as the H_2 gas in the synthetic air (dry air, no humidity, 79.1% N_2 -20.9% O_2) was inserted and stopped, following several cycles. The film demonstrated sensing reversibility as this is illustrated in figure 5. Interruption H_2 gas flow lead to the recovery of the prior sensing element electrical resistance. The reproducibility of the acquired results, supports the credibility of our sensing element performance and reliability. The sensing film demonstrated a reversible sensing behaviour under various hydrogen gas concentrations: 100, 75, 50, 25 and 10 ppm. As a result, the reducing gas causes an increase in the film resistance, reconfirming its p-type character.

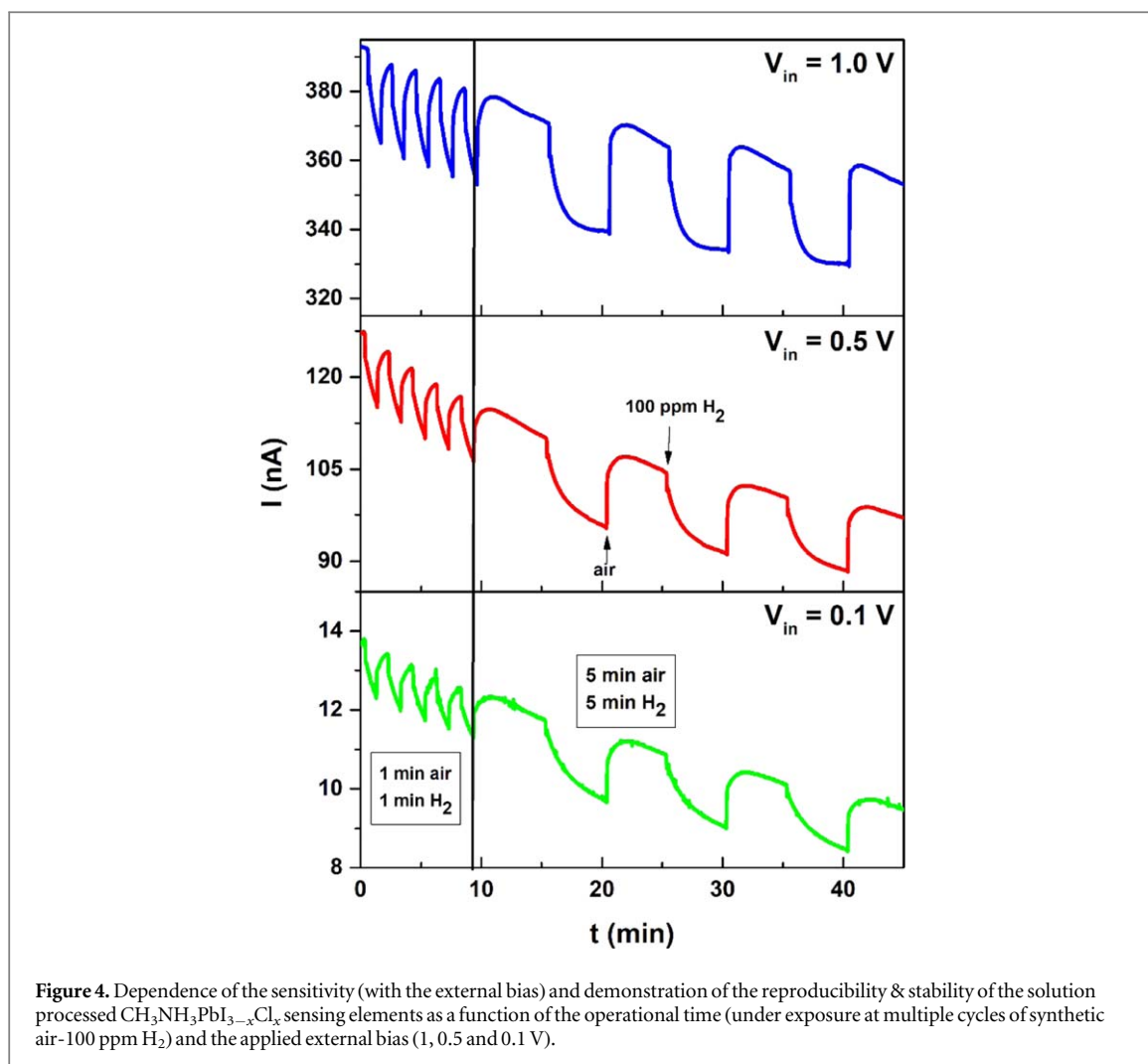


Figure 4. Dependence of the sensitivity (with the external bias) and demonstration of the reproducibility & stability of the solution processed $CH_3NH_3PbI_{3-x}Cl_x$ sensing elements as a function of the operational time (under exposure at multiple cycles of synthetic air-100 ppm H_2) and the applied external bias (1, 0.5 and 0.1 V).

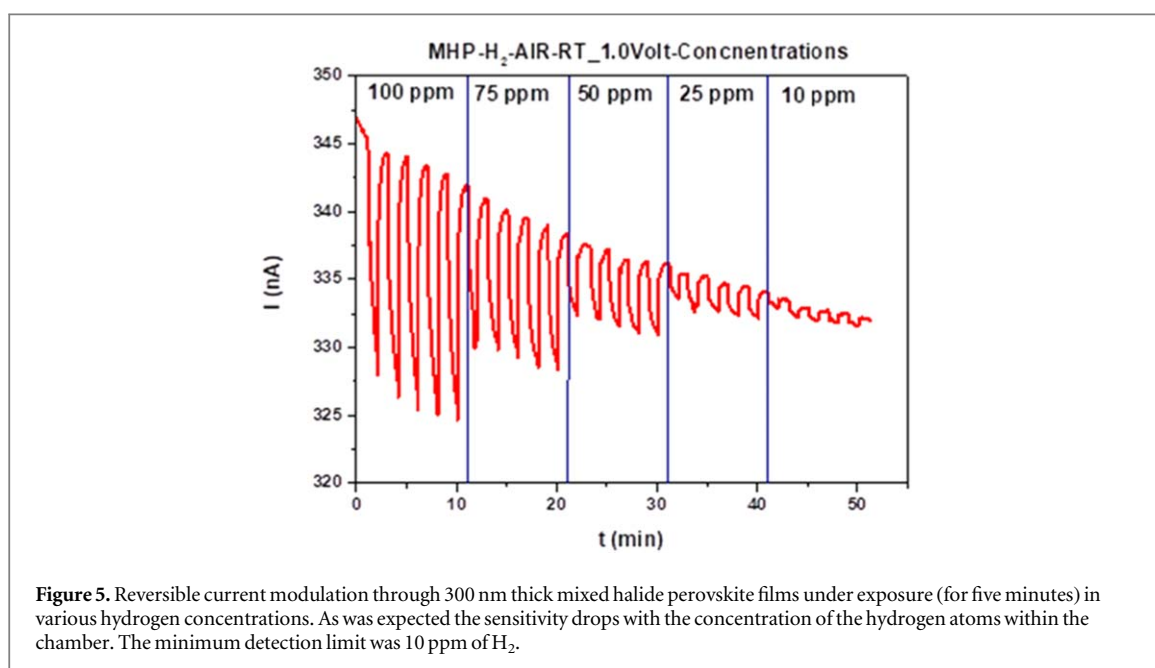


Figure 5. Reversible current modulation through 300 nm thick mixed halide perovskite films under exposure (for five minutes) in various hydrogen concentrations. As was expected the sensitivity drops with the concentration of the hydrogen atoms within the chamber. The minimum detection limit was 10 ppm of H_2 .

As expected, our perovskite sensing platform demonstrated different sensitivity at different targeted gas concentrations (figure 5). This, in combination with the abrupt increase of the resistance, was attributed to the H_2 molecules adsorption into the perovskite surface. Furthermore, as the need for low temperature gas sensors is

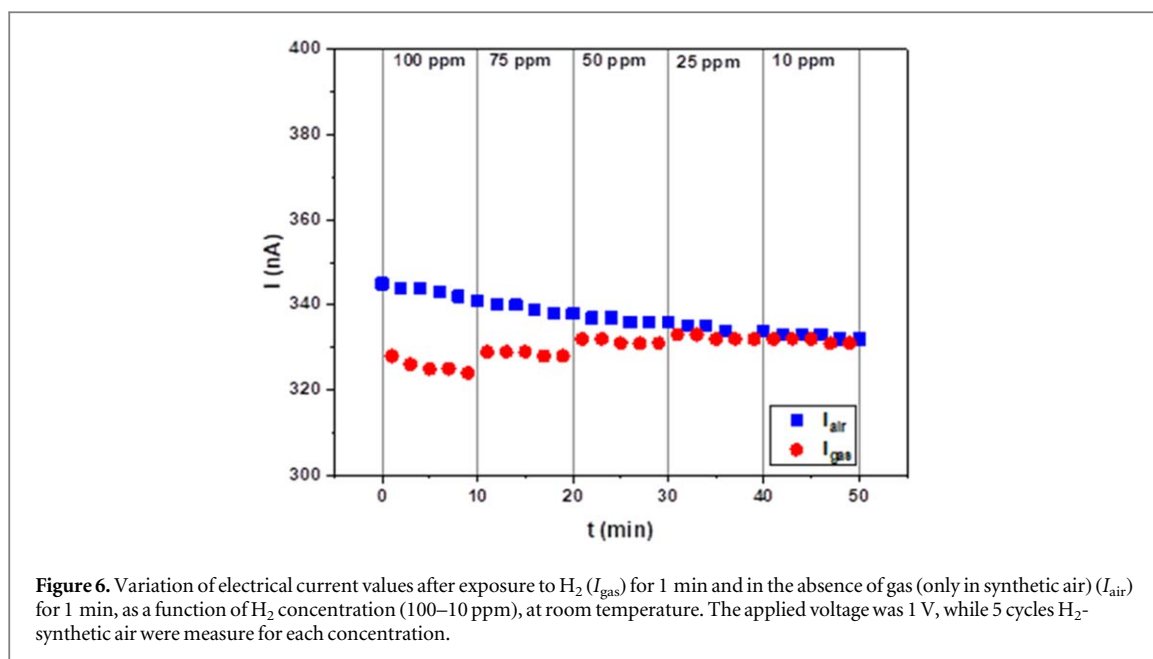


Figure 6. Variation of electrical current values after exposure to H₂ (I_{gas}) for 1 min and in the absence of gas (only in synthetic air) (I_{air}) for 1 min, as a function of H₂ concentration (100–10 ppm), at room temperature. The applied voltage was 1 V, while 5 cycles H₂-synthetic air were measure for each concentration.

Table 1. Calculated values of the electrical current values after exposure to H₂ (I_{gas}) for 1 min and in the absence of gas (only in synthetic air) (I_{air}) for 1 min sensitivity (S), response (t_{resp}) and recovery (t_{rec}) times of the demonstrated perovskite films under various H₂ gas concentration exposures.

H ₂ concentration (ppm)	I_{air} (nA)	I_{gas} (nA)	ΔI (nA)	S (%)	t_{resp} (s)	Mean t_{resp} (s)	t_{rec} (s)	Mean t_{rec} (s)
100	343.6	325.6	18	5.2	58.50		20.40	
75	339.6	328.6	11	3.2	44.58		23.04	
50	336.8	331.4	5.4	1.6	34.56	45.14	42.48	35.40
25	334.8	332.4	2.4	0.7	49.56		30.00	
10	332.6	331.6	1	0.3	38.52		61.08	

becoming a necessity and moreover for safety reasons in the case of the highly flammable H₂ gas, all the measurements were taken at room temperature although sacrificing part of the response signal obtained at elevated temperatures. All the measurements were recorded until the current through the sample had reached its lowest value. The observed drifting of the background current as a function of time was attributed (a) to remaining trapped H₂ molecules within our sensing platform and (b) a probable degradation of the sensing element. This process duration was lasted for approximately five minutes after which no further substantial changes were observed. The sensing measurement was repeated under each hydrogen gas concentration for five times (five cycles) (figure 5), showing excellent reproducibility. The sensing ability was assessed with the measurement of (a) the sensitivity (S); and (b) the response & recovery times of the film. The sensitivity parameter is calculated using the following formula (1) [43]

$$S(\%) = \frac{|I_{\text{air}} - I_{\text{gas}}|}{I_{\text{air}}} 100\%, \quad (1)$$

where I_{air} denotes the electrical current of the sensor before the exposure into the H₂ environment, I_{gas} the resistance of the sensor after ten minutes to hydrogen. The lower exhibited sensitivity from the perovskite sensing element compared to these ones the metal oxides demonstrated (~80% at RT, for 100 ppm H₂) [16, 20] is among the disadvantages the former materials are characterised. More work has to be done in order to improve this sensing parameter. The response (t_{resp}) and the recovery (t_{rec}) times were calculated as the times take the measured current to reach the 10% of its maximum value under H₂ exposure and 90% of its maximum value under synthetic air environment (H₂ gas flow has been interrupted), respectively. The response and recovery times demonstrated almost identical average values, 45 and 35 s, respectively. The dependence of electrical current values after exposure to H₂ (I_{gas}) for 1 min and in the absence of gas (only in synthetic air) (I_{air}) for 1 min, as a function of H₂ concentration (100–10 ppm), at room temperature is depicted on figure 6.

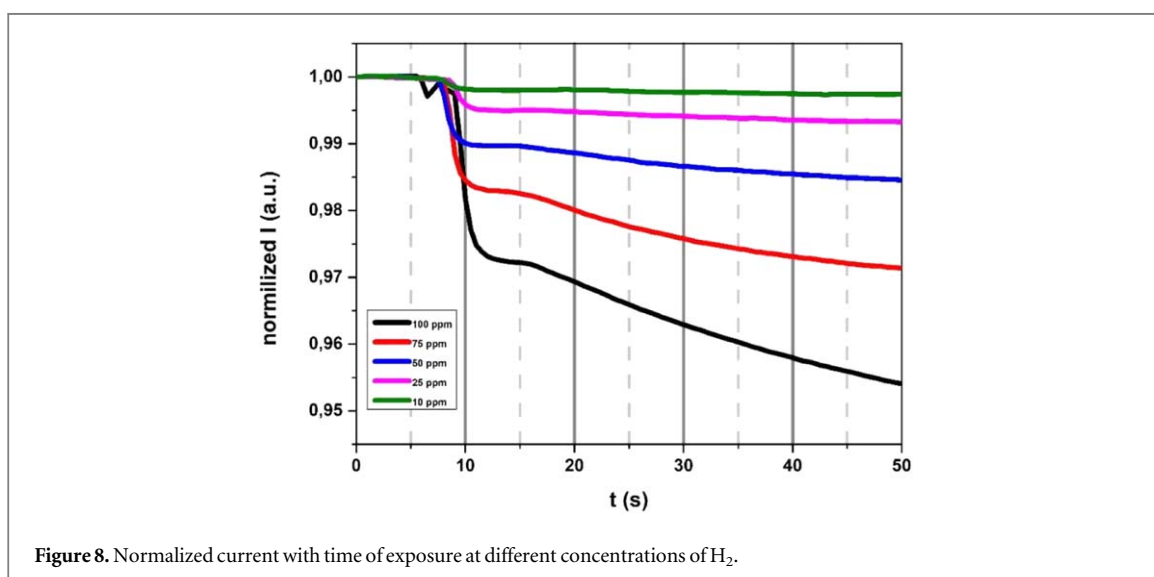
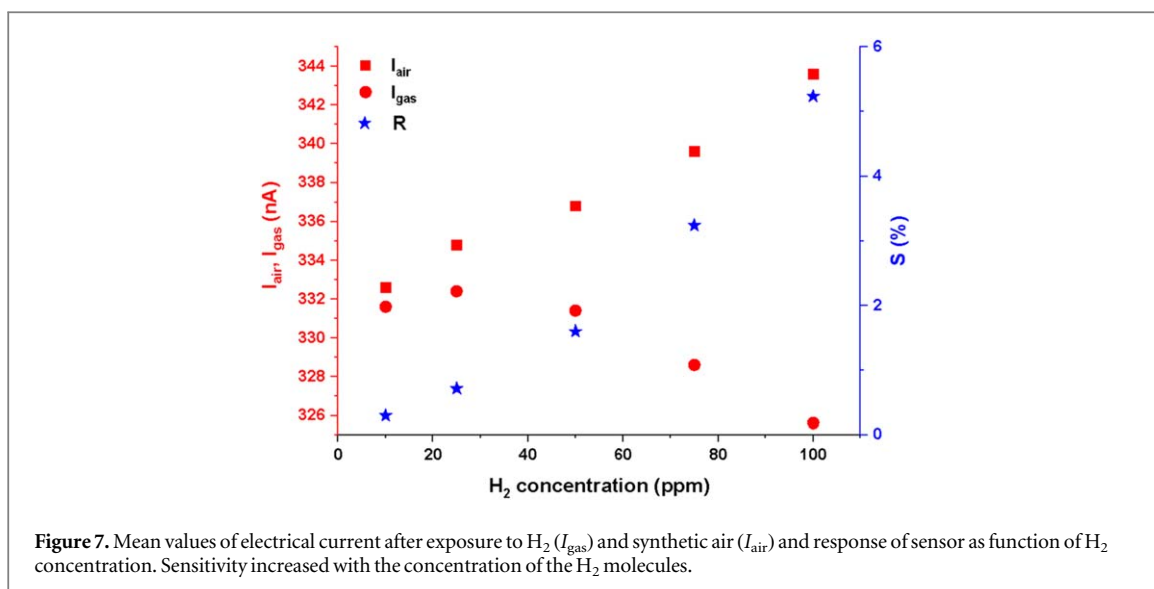
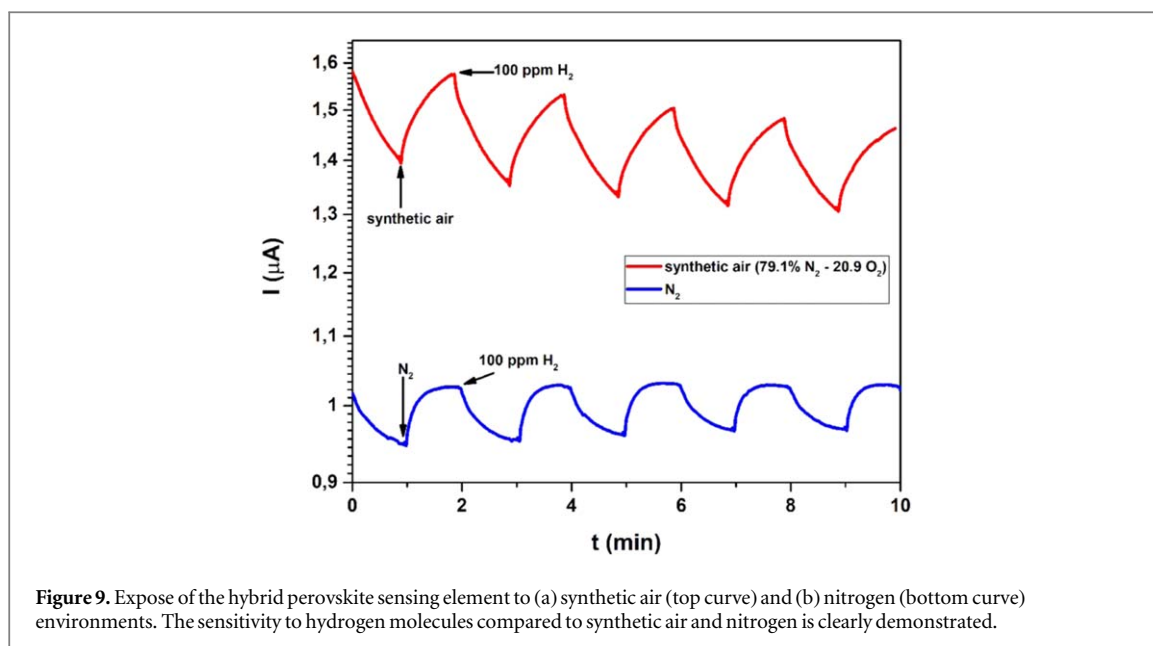


Table 1 presents all the calculated values, extracted from the measurements depicted on figure 6, under the different H₂ gas concentrations taken. All these values have been plotted and illustrated on figure 7.

The fast sensing response of the exhibited films allowed the distinction of the various H₂ concentrations. You can see in figure 8 below, that the maximum exposure time in order to distinguish the different H₂ concentrations was 10 s.

The absence of any phase transformation and impurity formation, upon exposure to a H₂ atmosphere, shows the non-chemical interaction of the hydrogen with the halide perovskite platform. This is also supported from the reversibility of the electrical properties of the perovskite-based film exhibited after the removal of the H₂ gas molecules from the chamber. It is profound that the H₂ molecules are adsorbed through the porous of the perovskite film and bond loosely with its crystal template close to the surface; this can be interpreted by the small response and recovery times the film showed. The increase of the films' resistance under the H₂ exposure (a reduction gas) indicate the introduction of electrons to the halide perovskite platform. These electrons recombine with the holes (majority charge carriers in the p-type semiconductor) and result in the lowering of the current through the film. We attribute the donation of the electrons to the perovskite platform to the following mechanism: Firstly, neutral oxygen molecules (the most probable from the synthetic air existed within the vacuum chamber) are adsorbed into the perovskite platform and convert into oxygen ions: O₂⁻, O⁻ and O²⁻ ions by attracting electrons from the semiconductor valence band. Subsequently, the hydrogen atoms interact with these oxygen ions, producing water with the simultaneous release of electrons. The latter recombine with the perovskite holes in the valence band and result in the observed enhancement of the film's resistance. When



hydrogen is desorbed, the surface of the material continues to adsorb oxygen from the environment to generate oxygen ions. At this time, the resistance of the material returns to the base value. To support this sensing mechanism, sensing experiments using different gas environments were performed. Pure nitrogen and synthetic air environments were tested. The sensing preference to hydrogen is clearly illustrated in figure 9, where the presented sensing element was exposed to (a) synthetic air; and (b) to nitrogen environment. The exposure of our sensing element to nitrogen environment or synthetic air demonstrated no interaction with the background environment.

However, the XRD measurements showed no compositional changes (the formation of water molecules should lead to a severe degradation and decomposition of the halide perovskite). This does not occur even though the films were exposed to H_2 environment for more than an hour. This is an open question. We conclude that further studies and theoretical modelling should be done to support further the aforementioned operational mechanism for the H_2 sensing.

It is noted that after a number of successive cycles, the current did not fully return to its initial value. This is attributed possibly to residual adsorbed H_2 molecules due to slight changes in the film's morphology as the AFM measurements revealed. The observation of no compositional change after the exposure to H_2 molecules is attributed to the good crystallinity of the perovskite film that reflects film's good stability. Moreover, the sensing properties in successive hydrogen/synthetic air switching cycles of the mixed halide films was tested after three weeks of storage under vacuum within the measurement chamber demonstrating remarkable sensing element durability. The results were encouraging, with the sensing element to demonstrate a good stability (see figure 10), as the sensitivity and the detected currents remained almost the same after three weeks of storage.

The ability to distinguish different gases was also demonstrated by the fabricated films. The same film exposed to the H_2 gas, was exposed to ozone molecules (figures 11(a) and (b)). The latter lowered the resistance of the films. The opposite result in the electronic properties of the same sensing platform the two different gases produced, accompanied with the different calculated sensitivities (in the case of ozone exposure the perovskite film demonstrated much better sensitivities), revealed the ability of the mixed halide perovskite films to distinguish two different gases.

The solution process ability and the crystallization of the employed perovskite in low temperatures, permitted the deposition of sensing active onto flexible e.g. PET substrates where similar electrode patterns with these films on rigid substrates have been printed. The film was exposed to H_2 environment under (a) no bending; and (b) bending conditions. In figures 12(a)–(c) is depicted the sensing performance under bending conditions (figure 12(b)); and the two extreme cases of no bending and bending close to 180° (figure 12(c)); in both cases the modulation of current due to H_2 interaction with the perovskite template could be detected and be measured. This is the first time that a report on the flexibility of the tested material as sensor is made and these results are very promising. The sensitivity recorded was comparable (around 7% under bending and exposed to 100 ppm of hydrogen molecules) with the one of the mixed halides films deposited onto glass substrates.

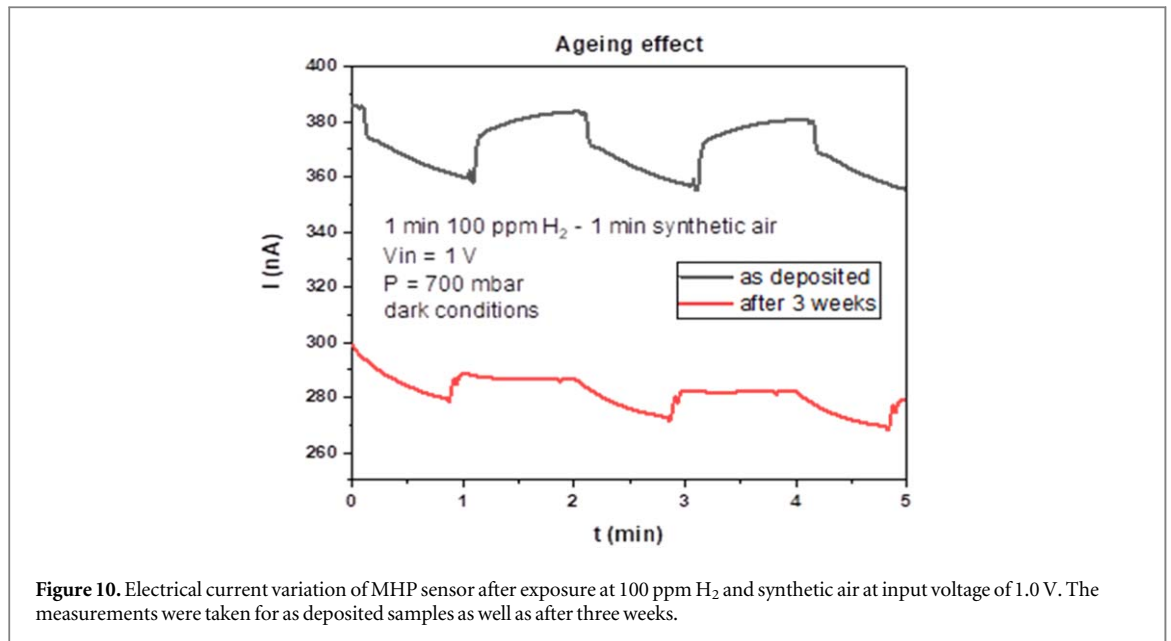


Figure 10. Electrical current variation of MHP sensor after exposure at 100 ppm H₂ and synthetic air at input voltage of 1.0 V. The measurements were taken for as deposited samples as well as after three weeks.

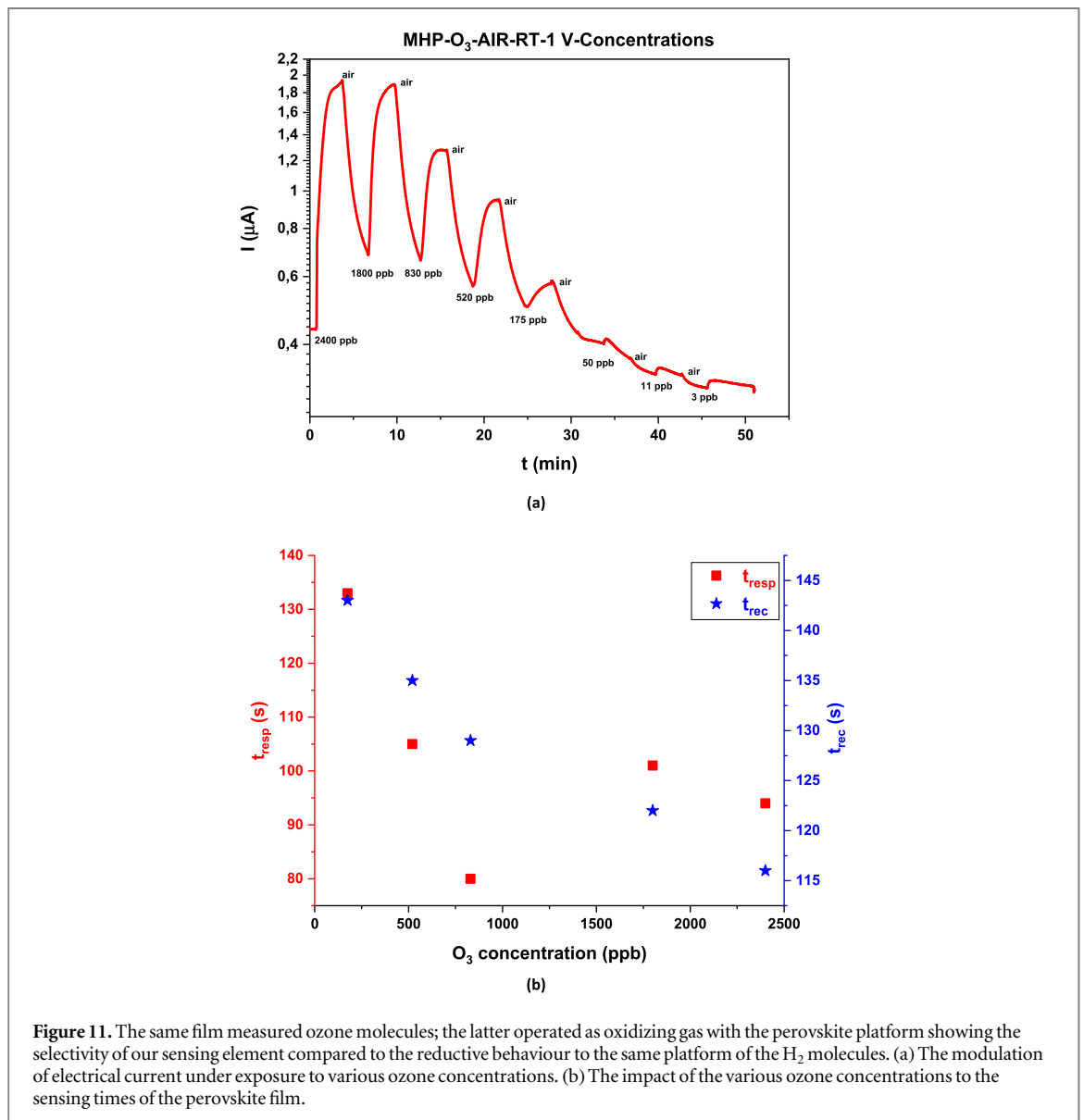
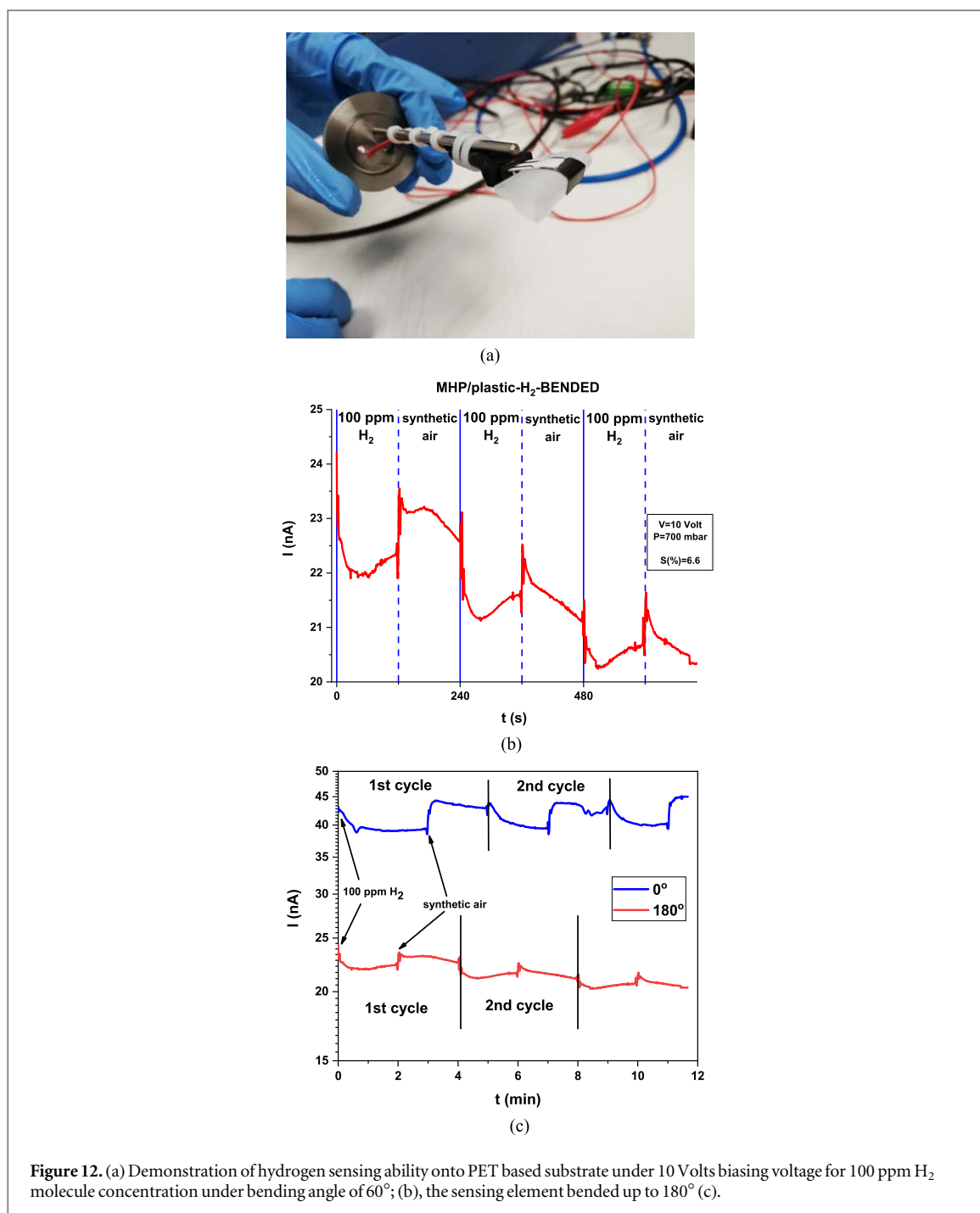


Figure 11. The same film measured ozone molecules; the latter operated as oxidizing gas with the perovskite platform showing the selectivity of our sensing element compared to the reductive behaviour to the same platform of the H₂ molecules. (a) The modulation of electrical current under exposure to various ozone concentrations. (b) The impact of the various ozone concentrations to the sensing times of the perovskite film.



4. Conclusions

We report, for the first time, to the best of our knowledge, a solution processed hybrid mixed halide perovskite films ($\text{CH}_3\text{NH}_3\text{PbI}_{3-x}\text{Cl}_x$) as hydrogen gas sensor elements. The films were prepared and spin coated onto rigid (glass) and flexible (PET), prepatterned with interdigitated electrodes, substrates. All films operated as self-powered sensing elements for H₂ at room temperature. Their sensing properties were based on modulations of its electrical resistance. H₂ sensing measurements revealed very promising results regarding the potential of this material as H₂ sensing element; the p-type semiconductor characterised by maximum sensitivities of the order of 5%–7%, with very fast reaction times of the order of few seconds and the capability to be able to distinguish between two different tested gases (H₂ and O₃). The compatibility of the demonstrated sensing element with flexible substrates was also confirmed. Ageing measurements showed that the devices retained their sensing abilities even after three weeks of storage. The observed lowering of the detecting current after each sensing cycle is a challenge to be tackled in the future. More experiments should be implemented to improve the lifetime of this sensing materials and increase the number of sensing cycles or the total exposure time to H₂. We believe that

the lifetime can be prolonged using composites of hybrid perovskites with graphene-based materials. The latter, will be placed between the grain boundaries of perovskite grains, due to their excellent conductivity will reduce the electrical stressing the perovskite platform experiences after each sensing cycle. However, despite the first promising results obtained, further work is planned be done in order to improve mixed halide perovskite film's sensing performance towards H₂ gas molecules. First of all, the operational mechanism should be confirmed and studied further. Second, doped hybrid perovskite mixed halide films or nanocomposites with graphene-based materials that exhibit higher conductivities, should be tested. The impact of higher conductivities to the sensing performance must be linked. This is expected to enhance the acquired sensitivity. Another idea, is to try to apply 2D solution processed perovskite materials since the lowering of dimension leads to higher surface to volume ratio and thus to the enhancement of all the figures of merit of a sensor: (a) higher sensitivities; (b) broader limit of detection; (c) higher stabilities. The better engineering of mixed halide perovskite probably will provide more tolerant to ion migration problem and will allow the application of higher applied voltages. This is expected to elevate the sensitivity of the particular sensing elements. Stimulated emission Raman Spectroscopy principles will be employed as a tool to be able to distinguish the various gases *in situ*.

Based in the above, it may be concluded that the hybrid mixed halide perovskite films could be a promising self-powered p-type sensing material for reducing gases as H₂ at room temperature.

Acknowledgments

Part of this work was supported by the project 'National Research Infrastructure on nanotechnology, advanced materials and micro/nanoelectronics' (MIS 5002772), as well as by the action 'QUALITY of LIFE' (MIS 5002464) both of which are implemented under the 'Action for the Strategic Development on the Research and Technological Sector' funded by the Operational Programme 'Competitiveness, Entrepreneurship and Innovation' (NSRF 2014-2020) and co-financed by Greece and the European Union (European Regional Development Fund).

Notes

The authors declare no competing financial interest.

ORCID iDs

E Gagaoudakis  <https://orcid.org/0000-0002-0567-0295>

References

- [1] Sanger A, Kumar A and Chandra R 2016 Highly sensitive and selective hydrogen gas sensor using sputtered grown Pd decorated MnO₂ nanowalls *Sensors Actuators B* **8** 234
- [2] Yoon K J, Lee S I, An H, Kim J, Son J W, Lee J H, Je H J, Lee H W and Kim B K 2014 Gas transport in hydrogen electrode of solid oxide regenerative fuel cells for power generation and hydrogen production *Int. J. Hydrog. Energy* **39** 3868–78
- [3] Smotkin E S, Jiang J, Nayar A and Liu R 2006 High-throughput screening of fuel cells electrocatalysts *Appl. Surf. Sci.* **252** 2573–9
- [4] Hubert T, Boon-Brett L, Black G and Banach U 2011 Hydrogen sensors—a review *Sensors Actuators B* **157** 329–52
- [5] Buttner W J, Post M B, Burgess R and Rivkin C 2011 An overview of hydrogen safety sensors and requirements *Int. J. Hydrog. Energy* **36** 2462–70
- [6] Aroutiounian J S 2005 Hydrogen detectors *Int. Sci. J. Altern. Energy Ecol.* **3** 21–31
- [7] Lith J V, Lassesson A, Brown S A, Schulze M, Partridge J G and Ayesh A 2007 A hydrogen sensor based on tunnelling between palladium clusters *Appl. Phys. Lett.* **91** 181910
- [8] Simon I and Arndt M 2002 Thermal and gas-sensing properties of a micromachined thermal conductivity sensor for the detection of hydrogen in automotive applications *Sensors Actuators A* **97–98** 104–8
- [9] Hübert T, Boon-Brett L, Black G and Banach U 2011 Hydrogen sensors—a review *Sensors Actuators B* **157** 329–52
- [10] Zhao F et al 2017 A novel versatile microbiosensor for local hydrogen detection by means of scanning photoelectrochemical microscopy *Biosens. Bioelectron.* **94** 433–7
- [11] Fisser M, Badcock R A, Teal P D and Hunze A 2018 Optimizing the sensitivity of palladium-based hydrogen sensors *Sensors Actuators B* **259** 10
- [12] Ganzha V et al 2018 Measurement of trace impurities in ultra-pure hydrogen and deuterium at the parts-per-billion level using gas chromatography *Nucl. Instrum. Methods Phys. Res. A* **880** 181–7
- [13] Podlepetsky B, Nikiforova M and Kovalenko A 2018 Chip temperature influence on characteristics of MISFET hydrogen sensors *Sensors Actuators B* **254** 1200–5
- [14] Ytsma C R and Dyar M D 2018 Effects of univariate and multivariate regression on the accuracy of hydrogen quantification with laser-induced breakdown spectroscopy *Spectrochim Acta B* **139** 27–37
- [15] Moon J, Hedman H-P, Kemell M, Tuominen A and Punkkinen R 2016 Hydrogen sensor of Pd-decorated tubular TiO₂ layer prepared by anodization with patterned electrodes on SiO₂/Si substrate *Sensors Actuators B* **222** 190–7

- [16] Stamatakis M, Tsamakidis D, Brilis N, Fasaki I, Giannoudakos A and Kompitsas M 2008 Hydrogen gas sensors based on PLD grown NiO thin film structures *Phys. Status Solidi* **205** 2064–8
- [17] Haija M A, Ayesh A I, Sadiqa A and Katsiotis M S 2016 Selective hydrogen gas sensor using CuFe₂O₄ nanoparticle based thin film *Surf. Sci.* **369** 443
- [18] Zhang D, Sun Y, Jiang C and Zhang Y 2017 Room temperature hydrogen gas sensor based on palladium decorated tin oxide/molybdenum disulfide ternary hybrid via hydrothermal route *Sensors Actuators B* **242** 15
- [19] Wu C-H, Zhu Z, Huang S-Y and Wu R-J 2019 Preparation of palladium-doped mesoporous WO₃ for hydrogen gas sensors *J. Alloys Compd.* **776** 965–73
- [20] Gagaoudakis E, Michail G, Kampylafka V, Tsagaraki K, Aperathitis E, Moschovis K, Binas V and Kiriakidis G 2017 Room temperature p-type NiO nanostructure thin film sensor for hydrogen and methane detection *Sensor Lett.* **15** 1–5
- [21] Weber M, Kim J-Y, Lee J-H, Kim J-H, Iatsunskyi I, Coy E, Miele P, Bechelany M and Kim S S 2019 Highly efficient hydrogen sensors based on Pd nanoparticles supported on boron nitride coated ZnO nanowires *J. Mater. Chem. A* **7** 8107–16
- [22] Moller C K 1958 Crystal structure and photoconductivity of Cæsium plumbahalides *Nature* **182** 1436
- [23] Kojima A, Teshima K, Shirai Y and Miyasaka T 2009 Organometal halide perovskites as visible-light sensitizers for photovoltaic cells *J. Am. Chem. Soc.* **131** 176050–1
- [24] <https://nrel.gov/pv/assets/pdfs/best-research-cell-efficiencies.20190802.pdf>
- [25] Zhang W, Eperon G E and Snaith H J 2016 Metal halide perovskites for energy applications *Nat. Energy* **1** 16048
- [26] Stranks S D and Snaith H J 2014 Metal-halide perovskites for photovoltaic and light-emitting devices *Nat. Nanotechnol.* **10** 391–402
- [27] Brenner T M, Egger D A, Kronik L, Hodes G and Cahen D 2016 Hybrid organic–inorganic perovskites: low-cost semiconductors with intriguing charge-transport properties *Nat. Rev. Mater.* **1** 15007
- [28] Stylianakis M M, Maksudov T, Panagiotopoulos A, Kakavelakis G and Petridis K 2019 Inorganic and hybrid perovskite based laser devices: a review *Materials* **12** 859
- [29] Xu W et al 2019 Rational molecular passivation for high-performance perovskite light-emitting diodes *Nat. Photon.* **13** 418–24
- [30] Yuan M et al 2016 Perovskite energy funnels for efficient light-emitting diodes *Nat. Nanotechnol.* **11** 872
- [31] Mei F, Sun D, Mei S, Feng J, Zhou Y, Xu J and Xiao X 2019 Recent progress in perovskite-based photodetectors: the design of materials and structures *Adv. Phys. X* **4** 1592709
- [32] Fang Y, Dong Q, Shao Y, Yuan Y and Huang J 2015 Highly narrowband perovskite single-crystal photodetectors enabled by surface-charge recombination *Nat. Photon.* **9** 679
- [33] Zhu Z, Sun Q, Zhang Z, Dai J, Xing G, Li S, Huang X and Huang W 2018 Metal halide perovskites: stability and sensing-ability *J. Mater. Chem. C* **6** 10121–37
- [34] Kakavelakis G, Gagaoudakis E, Petridis K, Petromichelaki V, Binas V, Kiriakidis G and Kymakis E 2018 Solution processed CH₃NH₃PbI_{3-x}Cl_x perovskite based self-powered ozone sensing element operated at room temperature *ACS Sens.* **3** 135–42
- [35] Brintakis K, Gagaoudakis E, Kostopoulou A, Faka V, Argyrou A, Binas V, Kiriakidis G and Stratakis E 2019 Ligand-free all-inorganic metal halide nanocubes for fast, ultra-sensitive and self-powered ozone sensors *Nanoscale Adv.* **1** 2699–706
- [36] Wei H et al 2016 Sensitive x-ray detectors made of methylammonium lead tribromide perovskite single crystals *Nat. Photon.* **10** 333–9
- [37] Zhu Z, Sun Q, Zhang Z, Dai J, Xing G, Li S, Huang X and Huang W 2018 Metal Halide perovskites: stability and sensing ability *J. Mater. Chem. C* **6** 10121–37
- [38] Kymakis E, Panagiotopoulos A, Stylianakis M M and Petridis K 2019 Organometallic Hybrid Perovskites for humidity and gas sensing applications *2D Nanomaterials for Energy Applications* (London: Elsevier) Ch 5 (under publication) *Nanomater. Energy Appl.*
- [39] Bala A, Majumder S B, Dewan M and Chaudhuri A R 2019 Hydrogen sensing characteristics of perovskite-based calcium doped BiFeO₃ thin films *Int. J. Hydrog. Energy* **44** 18648–56
- [40] Huang W, Li Y, Ding Y and Li H 2019 Preparation and conductive properties of double perovskite Ba₃Sr_{1+x}Ta_{2-x}O_{9-δ} and application for hydrogen sensor *J. Alloys Compd.* **792** 759–69
- [41] Cui P, Wei D, Ji J, Huang H, Jia E, Dou S and Li M 2019 Planar p–n homojunction perovskite solar cells with efficiency exceeding 21.3% *Nat. Energy* **4** 150–9
- [42] Li Y, Sun W, Yan W, Ye S, Peng H, Liu Z, Bian Z and Huang C 2015 High performance planar solar cells based on CH₃NH₃PbI_{3-x}Cl_x perovskites with determined chlorine mole fraction *Adv. Funct. Mater.* **25** 4867
- [43] Steinebach H, Kannan S, Rieth L and Solzbacher F 2010 H₂ gas sensor performance of NiO at high temperatures in gas mixtures *Sensors Actuators B* **151** 162